

# Effect of compatibilizer concentration and weight fraction on model immiscible blends with interfacial crosslinking

Candice DeLeo

*Department of Chemical Engineering, University of Pittsburgh,  
Pittsburgh, Pennsylvania 15261 and Mascaro Center for Sustainable Innovation,  
University of Pittsburgh, Pittsburgh, Pennsylvania 15261*

Katie Walsh

*Department of Chemical Engineering, University of Pittsburgh,  
Pittsburgh, Pennsylvania 15261*

Sachin Velankar<sup>a)</sup>

*Department of Chemical Engineering, University of Pittsburgh,  
Pittsburgh, Pennsylvania 15261 and Mascaro Center for Sustainable Innovation,  
University of Pittsburgh, Pittsburgh, Pennsylvania 15261*

(Received 13 July 2010; final revision received 27 February 2011;  
published 12 April 2011)

## Synopsis

Reactive compatibilization, in which a compatibilizer is formed by an interfacial coupling between two reactive polymers, is commonly used when blending immiscible homopolymers. We consider reactive compatibilization using two multifunctional reactive polymers, which leads to a crosslinked copolymer at the interface. Experiments were conducted on model blends of polydimethylsiloxane (PDMS) and polyisoprene (PI). Compatibilizer was formed by a chemical reaction between amine-functional PDMS and maleic anhydride-functional PI. Droplet-matrix blends with a PI:PDMS ratio of 30:70 or 70:30 and reactive compatibilizer loadings from 0.1% to 3% were examined by optical microscopy and rheometry. Experiments reveal that the effects of interfacial crosslinking are highly asymmetric, with PI-continuous blends showing altogether different behaviors from PDMS-continuous blends. The PI-continuous blends show unusual features including drop clusters and nonspherical drops. In contrast, PDMS-continuous blends displayed a typical droplet-matrix morphology with round drops that do not appear to stick together. The rheological properties are also asymmetric: The PI-continuous blend showed gel-like behavior in oscillatory experiments, high viscosity, and viscosity overshoots during startup of shear flow, whereas PDMS-continuous blends showed liquidlike behavior that is qualitatively similar to that of compatibilizer-free blends. We speculate that the observed structural and rheological asymmetry is attributable to the asymmetry of the compatibilizer architecture on the two sides of the interface. © 2011 The Society of Rheology. [DOI: 10.1122/1.3571549]

---

<sup>a)</sup>Electronic mail: velankars@gmail.com

## I. INTRODUCTION

Compatibilizers are commonly used to promote blending of immiscible homopolymers. Numerous studies of immiscible blends have used premade diblock copolymers, principally because the structure of the compatibilizer is known precisely, and the amount of compatibilizer present in the blend can be controlled exactly. However, industrially it is much more common to generate a compatibilizer by an interfacial chemical reaction between two reactive polymers, each added to one of the two phases with which it is thermodynamically miscible [Datta and Lohse (1996); Koning *et al.* (1998); Baker *et al.* (2001)]. The reactive groups then arrive at the interface by diffusion, usually aided by the flow applied by the blending operation, resulting in compatibilizer formation at the interface. The structure of the two reactive species, their relative loadings, and the mixing procedure determine the architecture of the compatibilizer formed at the interface [DeLeo and Velankar (2008)]. The conceptually simplest situation is when both reactive species are monoendfunctional; in this case, a diblock copolymer is formed at the interface. Another simple case is when one polymer is monoendfunctional, whereas the other is multifunctional; in this case, a graft copolymer is formed at the interface.

This paper is chiefly concerned with the case of two multifunctional polymers so that a crosslinked compatibilizer can be formed at the interface. Many such examples of compatibilization using multifunctional reactive species can be found in the literature [Van Puyvelde *et al.* (1989); Weiss *et al.* (1989); Sundararaj *et al.* (1992); Beck Tan *et al.* (1996); Sun *et al.* (1998); Tselios *et al.* (1998); Lin *et al.* (2005)]. For example, maleated polymers are commonly used for reactive compatibilization, and each polymer chain will generally bear numerous reactive maleic anhydride groups. Several similar examples have been cited by DeLeo and Velankar (2008) and in review articles and books [Datta and Lohse (1996); Koning *et al.* (1998); Baker *et al.* (2001)]. Yet, none of these articles discuss interfacial crosslinking, although Oshinski *et al.* [Oshinski *et al.* (1992); Oshinski *et al.* (1996)] mentioned the possibility of nylon-6-6 forming crosslinks when reacted with maleated elastomers. Apart from synthetic polymers, many naturally occurring polymers—such as cellulose, starch, and chitin—are highly multifunctional and especially likely to form interfacial crosslinks when blended with other multifunctional polymers. As such polymers become commonplace in an increasingly sustainable world [Mohanty *et al.* (2002)], the effects of multifunctional reactivity in polymer blends will become more important. This motivates our study of the effects of multifunctional reactive compatibilization.

Our research uses immiscible polymer blends of polyisoprene (PI) and polydimethylsiloxane (PDMS). These are considered “model” materials because they are liquid at room temperature, thus allowing long term flow experiments without thermal degradation. Furthermore, they are nearly Newtonian, and hence any rheological complexity of the blends can be unambiguously attributed to the two-phase structure and to interfacial phenomena. Using these model blends, we previously compared the effect of multifunctional reactive compatibilization (which gives a crosslinked interface) against compatibilization with an added diblock copolymer [DeLeo and Velankar (2008)]. We showed that interfacial crosslinking caused unusual structural phenomena (drops that stick without coalescing and nonspherical drops) as well as strongly non-Newtonian rheology (gel-like behavior in small-amplitude oscillatory experiments, large overshoots in viscosity during startup of flow, and large strain recovery). That study was completed at a single composition (PDMS and PI in a 30:70 ratio) and a single compatibilizer loading (1.5 wt % of either the reactive compatibilizer or the diblock). Here, we examine the effects of varying the loading of the reactive compatibilizer. Furthermore, we also examine two different

TABLE I. Materials used.

Material	MW (g/mol)	$\eta_{25}^{\circ\text{C}}$ (Pa s)	Composition	Supplier
PI LIR30	29 000 <sup>a</sup>	131	100% PI	Kuraray
PI-MA	25 000 <sup>a</sup>	1700	1.5% MA <sup>a</sup>	Aldrich
PDMS	135 600 <sup>b</sup>	96	100% PDMS	Rhodia
PDMS*	5000 <sup>a</sup>	0.1	6–7% NH <sub>2</sub> <sup>a</sup>	Gelest
PI- <i>b</i> -PDMS	PI: 26 000; PDMS: 27 000		48% PI	

<sup>a</sup>Value quoted by supplier.

<sup>b</sup>Weight-average molecular weight estimated from known viscosity-MW relationship.

compositions: PDMS and PI in a 30:70 ratio (where PDMS forms the dispersed phase) or a 70:30 ratio (in which PI forms the dispersed phase). This latter comparison reveals surprising asymmetry in behavior depending on which phase forms the dispersed phase.

## II. MATERIALS AND METHODS

Various properties of all materials used are listed in Table I. The principal components of the blends are PI (Kuraray) and PDMS (Rhodia). PI is nearly monodisperse with a high 1,4-*cis* content, whereas PDMS is polydisperse. Both polymers are weakly viscoelastic liquids at room temperature: In small-amplitude oscillatory experiments, a significant storage modulus can be measured only at high frequencies, and in steady shear flow experiments shear-thinning is not evident at the stresses used in this work.

The chief concern of this paper is to investigate the effects of reactive compatibilizer that crosslinks at the interface of the two polymers. Reactively compatibilized blends were prepared by an interfacial chemical reaction between polyisoprene-graft-maleic anhydride (PI-MA) and poly(aminopropylmethylsiloxane-co-dimethylsiloxane) (PDMS-NH<sub>2</sub>). PI-MA has an (isoprene):(isoprene maleic anhydride) ratio of 98.5:1.5 and a molecular weight (MW) of 25 kg/mol, both quoted by the supplier, Aldrich. This corresponds to an average of  $\sim 5.5$  anhydride groups per PI-MA chain. PDMS-NH<sub>2</sub> is quoted by the supplier (Gelest) as having a molecular weight of 5 kg/mol and 6–7% of aminopropyl groups pendant from the chain; this corresponds to an average of 3.9–4.5 amine groups per chain. The material selection here is the same as in our previous publication [DeLeo and Velankar (2008)] with the exception of an increase in the PDMS-NH<sub>2</sub> functionality from 2–3 mol % in the previous paper to 6–7 mol % in the present paper.

One goal of this paper is to directly confirm copolymer formation at the interface by confocal microscopy. This necessitates tagging one of the reactive blocks by a fluorophore. For this purpose, we used 4-chloro-7-nitrobenzofurazan (commonly known as NBD chloride). While NBD chloride is itself not fluorescent, upon reacting with an amine, it forms a fluorescent species [Fager *et al.* (1973)]. In the present case, one quarter of the amine groups of PDMS-NH<sub>2</sub> (based on stoichiometry) were reacted with NBD chloride in a mutual solvent, dichloromethane, at room temperature. This reaction resulted in fluorescently tagged amino-functional PDMS, which is dubbed as \*PDMS-NH<sub>2</sub>.

In all blends, the two reactive species were present in an equal weight ratio, with the total compatibilizer loading (combining the weight of both reactive species) varying from 0.1 to 3.0 wt %. The ratio of the PDMS phase (PDMS+\*PDMS-NH<sub>2</sub>) to the PI phase (PI+PI-MA) was either 30:70 or 70:30. Samples will be designated by  $Sx-w_{comp}$ , where

**TABLE II.** Molecular characteristics of the components used.

	PI side	PDMS side
Homopolymer MW $M_H$ (g/mol)	29 000 <sup>a</sup>	135 600 <sup>b</sup>
Reactive species MW (g/mol)	25 000 <sup>a</sup>	5000 <sup>a</sup>
Reactive content of the reactive species		
on weight basis (mmol/g)	0.22	0.66 <sup>c</sup>
Reactive groups per reactive chain	5.5	3.3
Number of groups per chain that are expected to react <sup>d</sup>	5.5	1.1
MW of block (loop or tail) between reacted groups $M_B$ (g/mol) <sup>e</sup>	4390	2380
Number of monomers in each block (loop or tail) <sup>e</sup>	50	32
Ratio $M_H/M_B$	6.6	57

<sup>a</sup>Value quoted by supplier.

<sup>b</sup>Weight-average molecular weight estimated from known viscosity-MW relationship.

<sup>c</sup>This assumes that ~25% of the amine groups have been fluorescently tagged.

<sup>d</sup>The two reactive species are present in an equal weight ratio. However, the PDMS-NH<sub>2</sub> has three times as many reactive groups per gram than PI-MA. Therefore, all MA groups are expected to react, whereas an average of 33% of NH<sub>2</sub> groups are expected to react.

<sup>e</sup>Mean number based on stoichiometric calculations.

$x$  is the weight fraction of the PDMS phase and  $w_{comp}$  is the overall wt % of compatibilizer. For example, a 1 g sample of S30-3.0 contains 0.285 g PDMS, 0.685 g PI, and 0.015 g each of PI-MA and \*PDMS-NH<sub>2</sub>.

Some key information regarding the blends, in particular the reactive content in each of the two phases, is summarized in Table II. This table will be discussed in detail in Sec. IV, but here one salient point must be noted: Although the blends contain equal weight of the two reactive species, they are not stoichiometrically matched; the number of amine groups in the blends is approximately three times the number of available anhydride groups. Accordingly, if a complete reaction is assumed, all the anhydride groups will react, but only one third of the amine groups will react. Since there are an average of 3.3 amine groups per \*PDMS-NH<sub>2</sub> chain, each chain will react by an average of 1.1 times—a value only slightly larger than the minimum value of 1 required for crosslinking. Since our chief motivation is to examine crosslinked compatibilizers, it is crucial to first verify that the two species are actually capable of crosslinking when mixed in the 1:1 weight ratio.

To verify this, PI-MA and \*PDMS-NH<sub>2</sub> were each dissolved in toluene separately at 10 wt %. Then 0.5 g of each of these solutions was added to a vial and mixed together rapidly. The mixture immediately formed a gel [Fig. 1(a)]. This gel appears to show good elastic properties [Fig. 1(b)] even though it contains 90 wt % solvent. Upon evaporating the solvent, a tacky rubbery material was obtained which could be swollen, but not dissolved, in toluene. This experiment verifies that PI-MA and \*PDMS-NH<sub>2</sub> are indeed capable of crosslinking when mixed in a 1:1 weight ratio. More comments about the architecture of the crosslinked interface will be made in Sec. IV.

The blends were prepared in two steps. First, \*PDMS-NH<sub>2</sub> was mixed with the nonreactive PDMS, and PI-MA was mixed with the nonreactive PI in the appropriate ratios.

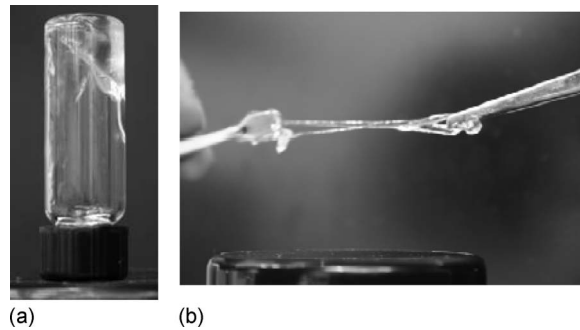


**FIG. 1.** (a) A gel formed from mixing together a 10% solution of PI-MA in toluene and 10% solution \*PDMS-NH<sub>2</sub> in toluene in a 1:1 ratio. The vial has been placed inverted to illustrate gelation. (b) The gel being stretched with tweezers.

Then these two phases were blended together in either a 30:70 or 70:30 weight ratio. All blends were mixed by hand using a spatula and degassed prior to further experiments.

Bright field microscopy was performed using an Olympus CKX41 inverted microscope equipped with a Basler area scan camera. Confocal microscopy was performed using an Olympus FluoView FV1000 inverted confocal microscope using an Ar-Ion laser at an excitation wavelength of 488 nm. Rheological experiments were performed using a TA Instruments AR2000 stress-controlled rheometer with 40 mm/1° cone and plate geometry, and the sample temperature of 25 °C was maintained using a Peltier cell.

### III. RESULTS AND DISCUSSION

#### A. Effect of compatibilizer concentration on morphology

This paper relies on an interfacial chemical reaction between PI-MA and \*PDMS-NH<sub>2</sub>. Labeling one of the reactive species (in the present case PDMS-NH<sub>2</sub>) with a fluorescent moiety offers an opportunity to verify the reaction visually (Fig. 2). In the absence of PI-MA (and therefore no possibility of interfacial coupling) the dispersed reactive PDMS forms droplets in the PI matrix [Fig. 2(a)]. These drops appear as uniformly bright fluorescent green spheres, indicating that \*PDMS-NH<sub>2</sub> is evenly mixed within the nonreactive PDMS causing the fluorescence to be distributed throughout the

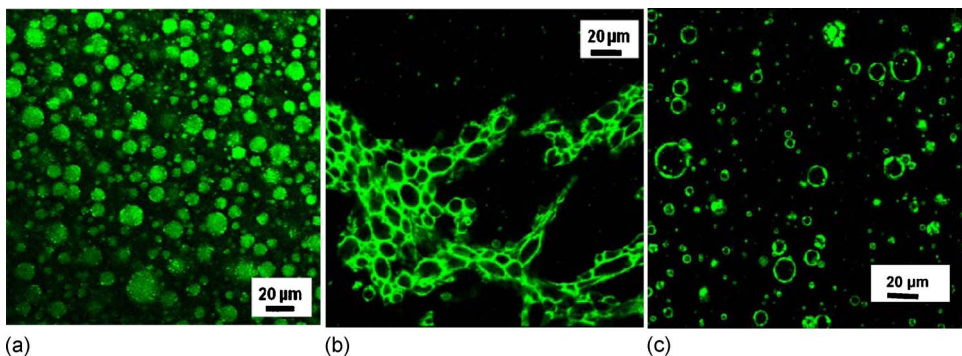


**FIG. 2.** The fluorescent images of (a) uncompatibilized S30-0 with \*PDMS-NH<sub>2</sub> but no PI-MA, and (b) S30-1.5 and (c) S70-3.0 clearly show that the reactive fluorescent species has moved to the interface. All images are colored in the online version.

drop. Upon the addition of small amounts of compatibilizer to S30 [Fig. 2(b)], the drop size begins to decrease and drops begin to cluster or stick together. The fluorescence is now localized at the interface and the drops are observed as bright green shells, suggesting that the amine/maleic anhydride chemical reaction has taken place. Moreover, the droplet shape becomes increasingly nonspherical. In the PDMS-continuous blend S70-3.0 [Fig. 2(c)] as well, the enhanced fluorescence at the interface as compared to the bulk confirms that the chemical reaction has indeed occurred. However, there is significant difference in the PI- and PDMS-continuous samples, viz., the droplets appear spherical and do not appear to stick together or form a network structure in the PDMS-continuous sample [Fig. 2(c)]. This will be discussed later in this paper.

S30 blends with reactive compatibilizer concentrations ranging from 0.1% to 3% of the total weight were examined by bright field microscopy. All blends of this composition were found to have PI as the continuous phase. Microscopic images are presented for S30-0.6 and S30-3.0 [Figs. 3(a) and 3(b)]. The morphologies of the blends were examined promptly after blending. The freshly blended samples were then allowed to sit under quiescent conditions for 24 h, and bright field microscopy was repeated. Immediately after blending S30-0.6 and S30-3.0, small PDMS drops were observed. Over 24 h of standing under quiescent conditions, the samples changed morphology significantly. At 0.6% compatibilizer loading, there appears to be a significant increase in drop size by coalescence, and the larger drops—many of which are nonspherical—appear to be fused together. In contrast, at 3% compatibilizer loading, there appears to be no significant change in the primary drop size; however, there is extensive aggregation of the drops. These effects are attributable [DeLeo and Velankar (2008)] to the interfacial chemical reaction which forms an interfacial “skin” covering the drops. This skin permits nonspherical drop shapes, as well as drop clustering without coalescence.

The microstructures of S70-0.6 and S70-3.0 are presented in Figs. 3(c) and 3(d). Upon mixing and after 24 h of quiescent conditions, a typical droplet-matrix morphology is evident, although the drop size appears larger in the S70 samples than in the corresponding S30 samples. Upon standing under quiescent conditions for 24 h, however, there are notable differences as compared to the S30 samples: All drops appear spherical, and clustering is not evident. [The nonspherical shapes in Fig. 3(c) are not drops suspended in the bulk; instead, they are drops that settled onto the glass slide and spread.] Several drops appear to grow in size, but other drops do not coalesce, suggesting that coalescence is slow, occurring over a time scale of days.

If these samples are allowed to sit under quiescent conditions for longer periods, the difference between the PDMS-continuous samples (e.g., S70-3.0) and the PI-continuous samples (e.g., S30-3.0) becomes evident even to the naked eye. The samples shown in Fig. 4 have been under quiescent conditions for several months. The S70-3.0 sample has undergone large-scale phase separation (the clear regions resulted from numerous coalescence events). The remaining regions, which are bright white, have a much smaller-scale two-phase structure. In contrast, the S30-3.0 sample undergoes much less phase separation with most of the regions of the Petri dish appearing bright white (indicating a phase separation on a length scale smaller than  $\sim 50 \mu\text{m}$ ). Even more importantly, there are regions of the Petri dish (indicated by the white arrows) that are not covered by the sample, indicating that S30-3.0 has a yield stress that prevents it from uniformly flowing over the bottom of the Petri dish. A similar observation was made in our previous article. In contrast, the S70-3.0 sample does not show such a bare region, but instead covers the bottom uniformly.

In summary, visualization results confirm that the interfacial reaction is occurring in both the S30 and S70 blends as evidenced by the bright interfacial regions in the confocal

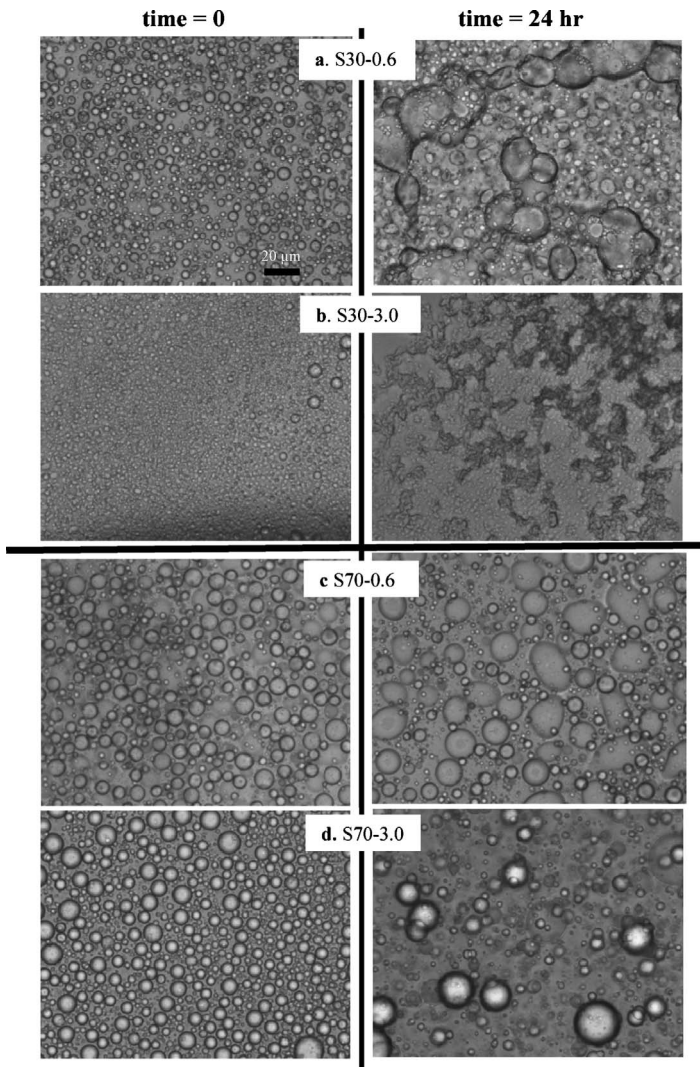


**FIG. 3.** Visualization of microstructure immediately after mixing ( $t=0$ ) and after 24 h at quiescent conditions. Droplet clusters increase with increasing reactive compatibilizer as shown by bright field microscopy by (a) S30-0.6 and (b) S30-3.0. The morphologies of (c) S70-0.6 and (d) S70-3.0 are not significantly affected by compatibilizer concentration. The scale bar of 20 micron shown in (a) applies to all images.

images. They also show that the effects of the reactively generated compatibilizer are highly asymmetric, both structurally (S70 blends show large round drops that can coalesce, whereas S30 blends show drops that can adopt nonspherical shapes and stick to each other) as well as rheologically (S30 blends show a yield stress whereas S70 blends do not). This asymmetry will also be apparent in the more quantitative rheological experiments of the next section.

## **B. Dynamic oscillatory properties**

### **1. Gel-like behavior at high compatibilizer loading**

Strain-sweep measurements were conducted at four different frequencies (100, 10, 1, and 0.1 rad/s) for strains ranging from 0.1% to 10%. All blends showed linear viscoelas-

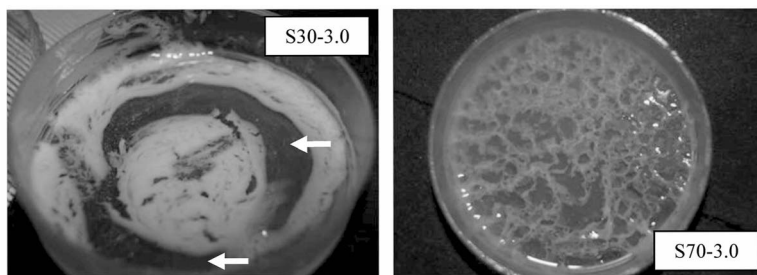
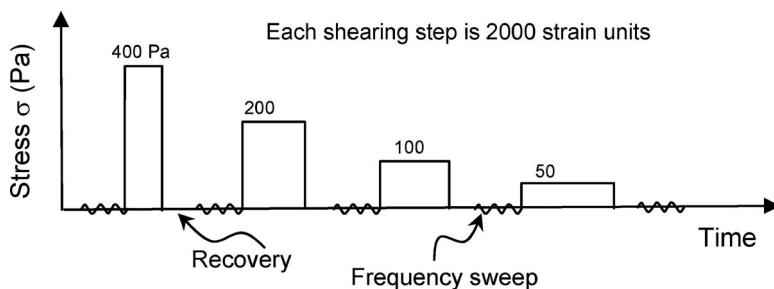


**FIG. 4.** Macroscopic images of S30 and S70 blends after several months of quiescent conditions. The white arrows point to large areas in which the bottom is bare, i.e., not covered by the polymer.

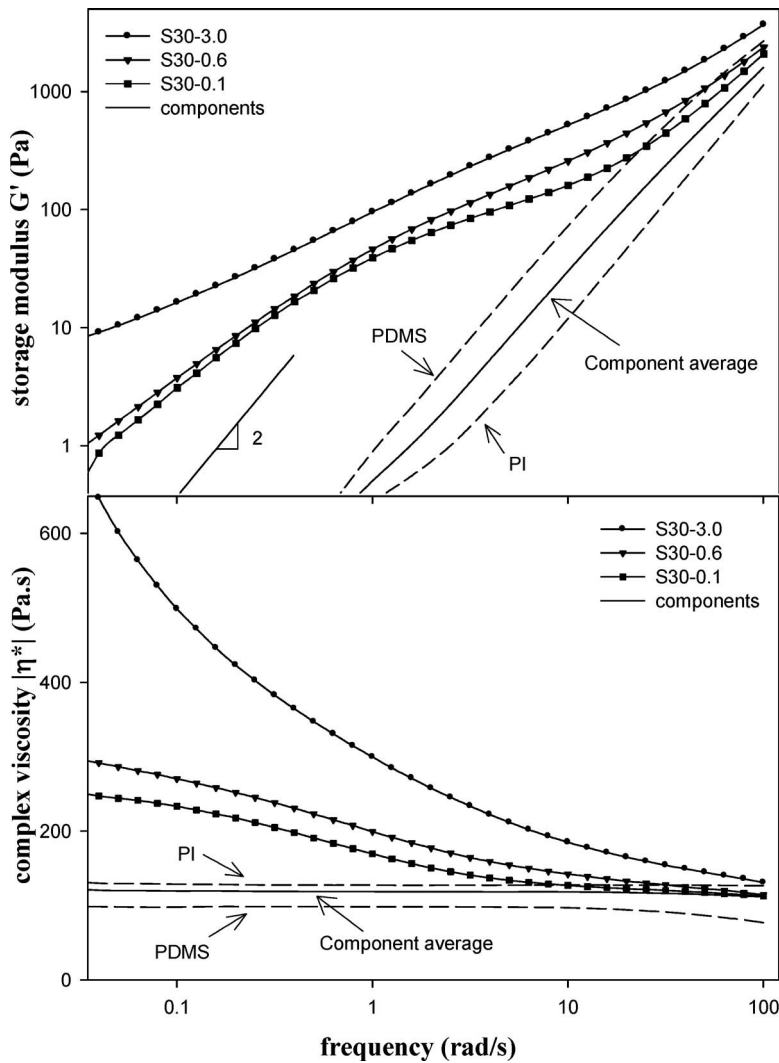
tic behavior under these conditions. All subsequent oscillatory measurements were conducted at 1% strain. The complete shear history of the rheological experiment is detailed in Fig. 5.

Figure 6 shows the oscillatory frequency sweeps of the as-prepared samples, i.e., the samples were tested immediately after degassing with no preshearing other than that experienced during sample loading. For clarity, only the S30-0.1, S30-0.6, and S30-3.0 blends are shown. The oscillatory behavior for the remaining blends closely resembled that of the three blends shown, in particular, S30-0 and S30-0.4 were similar to S30-0.1, S30-0.75 was similar to S30-0.6, and S30-1.5 was similar to S30-3.0. The behavior at low compatibilizer levels (0.4% and lower) resembles the behavior of the compatibilizer-free blends reported previously. In particular,  $G'$  and  $|\eta^*|$  show a pronounced shoulder at lower frequencies that has been attributed to interfacial relaxation processes, chiefly, relaxation of the drop shape [Oldroyd (1953); Paliarne (1990); Gramespacher and Meissner (1992); Vinckier *et al.* (1996)]. Furthermore, at the lowest accessible frequencies,  $G'$  scales with nearly the square of the frequency, and  $|\eta^*|$  nearly levels off, both of which are indicative of liquidlike behavior.

With increasing compatibilizer loading, the following changes occur: The shoulder in  $G'$  becomes less prominent, the slope of  $\log(G')$  vs  $\log(\text{frequency})$  increasingly deviates from a slope of 2 at low frequencies, and  $|\eta^*|$  shows an increasing trend with decreasing frequency. Such behavior is sometimes dubbed as gel-like [Doublier and Wood (1995); Ross-Murphy (1995); Thareja and Velankar (2006); Pozo *et al.* (2009)], although it does not obey the strict definition of a critical gel [ $G'$  and  $G''$  are both proportional to  $(\text{frequency})^\alpha$ , where  $\alpha$  is roughly 0.5] provided by Winter and Chambon (1986). Such behavior was already noted in our previous article using similar materials, and we had



**FIG. 5.** Shear history of the rheology experiment.



**FIG. 6.** As loaded oscillatory for varying compatibilizer concentrations in PI-continuous blends. The solid line is the volume-weighted average of the component homopolymers.

attributed it to the aggregation (without coalescence) of drops as evident in Fig. 2(b). With the additional compatibilizer loadings studied here, it is apparent that the gel-like behavior is not apparent at or below 0.4 wt % loading, but is highly pronounced at compatibilizer loadings exceeding 1.5 wt %.

The as-loaded oscillatory properties for the S70-3.0 compatibilizer are presented in Fig. 7, along with S70-0.6 and S70-0.1. At low compatibilizer loadings, the results resemble those of Fig. 6: The interfacial relaxation process is clearly evident, and the terminal region indicates liquidlike behavior. However, at higher compatibilizer loadings it is immediately apparent that the gel-like behavior is less prominent in S70-3.0 compared to S30-3.0. The oscillatory behavior of S70-3.0 appears more liquidlike and has a much smaller complex viscosity than S30-3.0. In effect, at the same compatibilizer load-

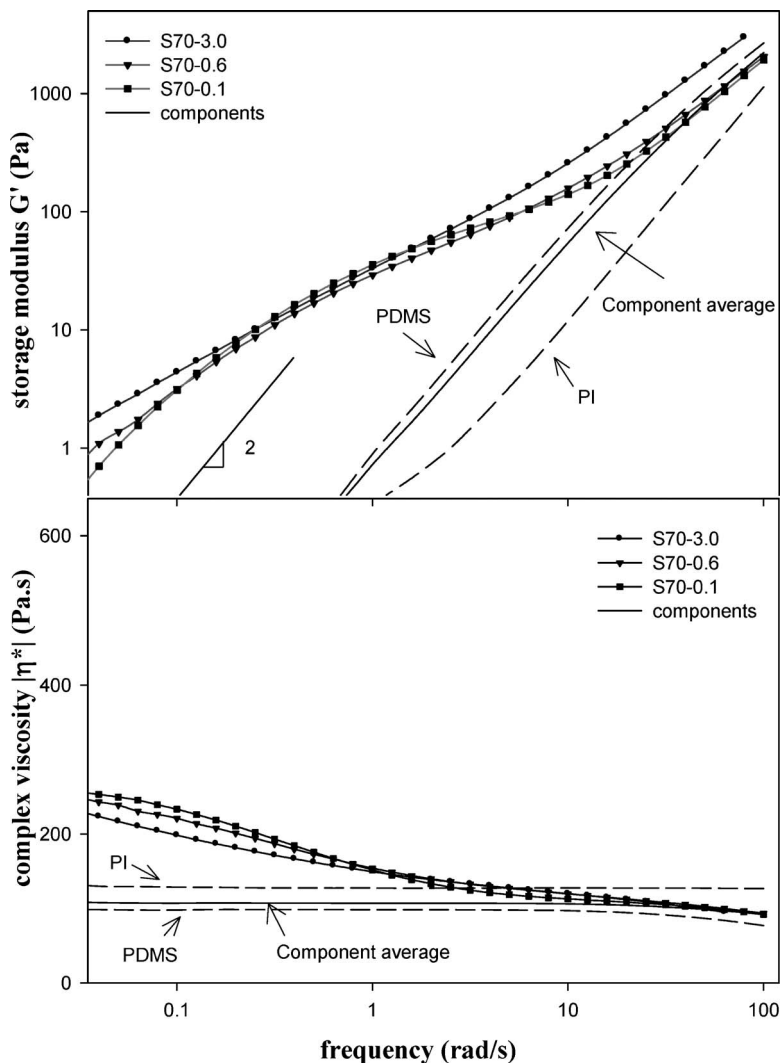
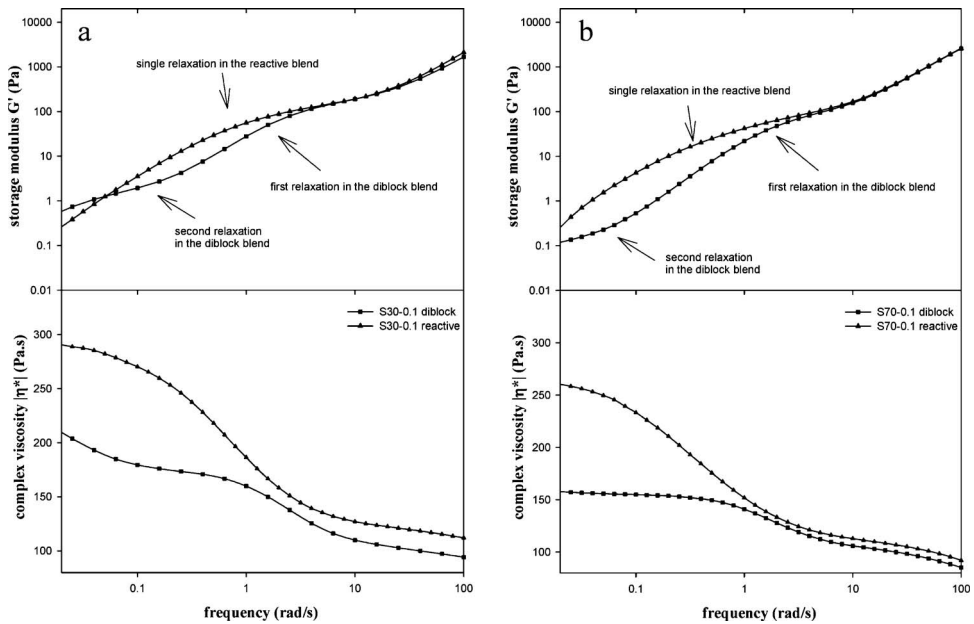


FIG. 7. As loaded oscillatory for varying compatibilizer concentrations in PDMS-continuous blends. The solid line is the volume-weighted average of the component homopolymers.

ing (3%), the rheological properties are qualitatively different depending on which phase is continuous. Such asymmetries are peculiar but not unique [Martin and Velankar (2007)] and will be discussed further in Sec. III C.

## 2. Low compatibilizer loadings: Comparison with diblock

Our previous article compared the reactive compatibilizer with a diblock compatibilizer at a single—and fairly high—compatibilizer loading. It is useful to make the same comparison at low compatibilizer loading, because diblock compatibilizers are known to show qualitatively different behaviors when the diblock loading is very low. Specifically, as the amount of diblock compatibilizer decreases to below roughly 0.5–1% the single relaxation process discussed in the previous paragraph splits into two: a higher frequency relaxation attributable to the deformation and relaxation of drops (“shape relaxation”),



**FIG. 8.** Diblock (squares) vs reactive blending (triangles); no second shoulder is apparent in  $G'$  or  $|\eta^*|$ , the reactive blends of (a) S30 and (b) S70.

and a new slower relaxation that has been attributed to interfacial viscoelasticity. The slow relaxation has been found to be nearly independent of drop size. With decreasing compatibilizer content, the slow relaxation moves to even lower frequencies until it is no longer observable in the accessible frequency range. With increasing compatibilizer content, the slow relaxation moves to higher frequencies until it merges with the shape relaxation and is not visible separately anymore. Further details of this slow relaxation have been discussed in several articles [Riemann *et al.* (1997); Jacobs *et al.* (1999); Van Hemelrijck *et al.* (2004); Van Hemelrijck *et al.* (2006); Friedrich and Antonov (2007)]. To summarize, blends compatibilized with low loadings of diblock copolymer can show two distinct relaxations, and it is of interest to examine whether the reactively compatibilized blend at low compatibilizer loading shows two relaxations as well.

Accordingly, we examined the blends with 0.1% compatibilizer in greater detail: The experiments with S30-0.1 and S70-0.1 were repeated, with the frequency sweep accessing lower frequencies. Figure 8 compares these data against the corresponding blends compatibilized with 0.1% diblock copolymer. This same diblock was used in our previous article [DeLeo and Velankar (2008)] and also by Van Hemelrijck *et al.* (2005). The diblock-containing blend was prepared in the same manner as the reactively compatibilized blends. It is clear from this figure that while the diblock-containing blends clearly show two relaxation processes, the reactively compatibilized blends do not.

This observation can be explained readily. Diblock compatibilizers lower the interfacial tension between immiscible homopolymers, and any dilation of the interface will raise the interfacial tension above the equilibrium value—an effect called dilational elasticity. If the interface is deformed nonuniformly (as is the case when drops are subjected to oscillatory shear), interfacial tension gradients result. It is the relaxation of interfacial tension gradients (via the spreading pressure of the diblock) that causes the slow relaxation [Oldroyd (1953); Jacobs *et al.* (1999); Friedrich and Antonov (2007)]. A crosslinked

interface on the other hand is solidlike and lacks mobility; concepts such as interfacial tension and spreading pressure do not readily apply to such solidlike interfaces. Thus, such an interface lacks dilational elasticity, interfacial tension gradients are not possible, and a slow relaxation is not observed.

### C. Steady shear characteristics

#### 1. Effect of lowering stress: Coalescence suppression

One important role of compatibilizer in droplet-matrix blends is coalescence suppression [Velankar *et al.* (2004)]. If coalescence is effectively suppressed, a finer morphology can result because the small drops created during the most intense portion of the blending process do not recombine in the less intense portions. The mechanism of coalescence suppression from the addition of a compatibilizer is not completely understood; however, two explanations are generally accepted to explain it [Van Puyvelde *et al.* (2001)]. First, coalescence suppression is a result of steric hindrance when two compatibilized drops approach each other [Macosko and Guegan (1996); Lyu *et al.* (2002)]. In this case, a higher molecular weight block will more efficiently suppress coalescence. Second, Marangoni stresses attempt to distribute the compatibilizer uniformly at the interface. As a result, when two drops approach each other, their interfaces become immobilized, greatly inhibiting the fluid in the gap from draining out and hence preventing coalescence [Miller and Xi (1996); Hu *et al.* (2000)].

As stated in Sec. III B, interfacial phenomena can give rise to clearly identifiable relaxation processes in dynamic oscillatory experiments. In compatibilizer-free blends, the only interfacial process is shape relaxation of the drops, and the time scale of this process (i.e., the reciprocal of the frequency of the shoulder in  $G'$ ) scales with the drop size. Accordingly, the changes in drop size can be followed quantitatively by changes in the shoulder in  $G'$ . The situation is more complex for compatibilized blends, and other interfacial processes (described in Sec. III B 2) can also play a role; nevertheless, the changes in the dynamic oscillatory properties are still qualitatively related to changes in drop size. Thus, dynamic oscillatory experiments are a convenient tool to probe coalescence phenomena. These experiments followed a shear step, followed by an oscillatory step to probe changes in drop size. Directly after the initial oscillatory measurements, the samples were subjected to the shear history of Fig. 5. The samples were sheared at 400 Pa for 2000 strain units, and then the subsequent recovery upon cessation of shear was monitored, followed by an oscillatory frequency sweep at 1% strain. This sequence (shear for 2000 strain units, recovery, and oscillatory) was repeated at successively lower stresses of 200, 100, and 50 Pa.

Figure 9 presents the oscillatory data recorded after shearing at 400 Pa and at 50 Pa for S30 and S70 samples containing various amounts of reactive compatibilizers. The data for the two intermediate shearing steps (200 and 100 Pa) fall between these lines in all cases. At 0.1% compatibilizer loading (as well as in the uncompatibilized sample, not shown), the interfacial relaxation process shifted to lower frequencies upon shearing the sample at lower stresses. The clearest indication of the shift is that  $G'$ 's at the two stresses now cross each other; in effect, upon shearing at low stress,  $G'$  increases at the lowest frequency, but decreases at intermediate frequencies. This slowing down of the interfacial relaxation is clearly evident in both the S30-0.1 and S70-0.1 samples and indicates a growth in drop size due to coalescence. At 0.6% and 3% compatibilizer loadings, however, the behavior of the S30 and S70 samples diverges. In the S70 samples, a small slowing down of the interfacial relaxation process is still evident, although it is not nearly as prominent as at 0.1% compatibilizer loading. In contrast, in the S30 samples, the

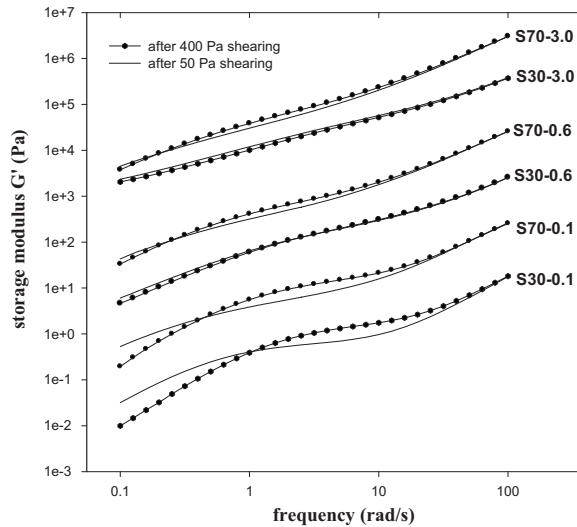


**FIG. 9.** Dynamic oscillatory properties after the 400 Pa shearing (symbols) and 50 Pa shearing (no symbols). They y-axis refers to the S30-0.1 blend. Every other dataset is shifted upwards by a factor of 10 with respect to the previous one for clarity.

slowing down is not evident (a crossover is not evident in the accessible frequency range). In summary, the oscillatory data after cessation of flow suggest that flow-induced coalescence is nearly suppressed in the S30 blends at compatibilizer levels exceeding 0.6%. In contrast, flow-induced coalescence is still possible in the S70 blends. This asymmetry of flow-induced coalescence appears to mirror the asymmetry of quiescent coalescence from optical microscopy (Sec. III A).

## 2. Creep behavior and steady shear viscosity

With the addition of any compatibilizer, all the steady shear viscosities of polymer blends are expected to increase as a result of the viscoelasticity of the interface [Velankar *et al.* (2004); Friedrich and Antonov (2007)]. In Fig. 6, the marked increase in the complex viscosity, especially at low frequency, suggests that there exists some compatibilization limit beyond which the material would become unprocessable. To examine the processibility of the blends, we examine the creep behavior of blends at various stress levels (Fig. 10).

Figure 10(a) shows the creep behavior of S30-3.0 and S70-3.0 at various stress levels. It is immediately apparent that the S30-3.0 blends show a large overshoot in the viscosity at short times. In contrast, S70-3.0 shows almost no overshoot at the three lower stress levels; only at the highest stress of 400 Pa (which is also the first steady-flow step) is an overshoot evident. In our previous study, a similar viscosity overshoot was seen for a similar S30 blend, and we showed that the overshoot is attributable to the aggregation of drops into clusters (as seen in Fig. 2). Earlier in this article we showed that drops of the S70 blends do not aggregate (they can only coalesce). Thus, the lack of a viscosity overshoot is consistent with the lack of aggregation.

Figure 10(b) plots the steady shear viscosity reached at long times at the various stress levels. The fact that these blends retain a modest viscosity under steady shear indicates that they remain processible, i.e., as a practical matter, as long as crosslinking is restricted to the interface, processibility is retained.

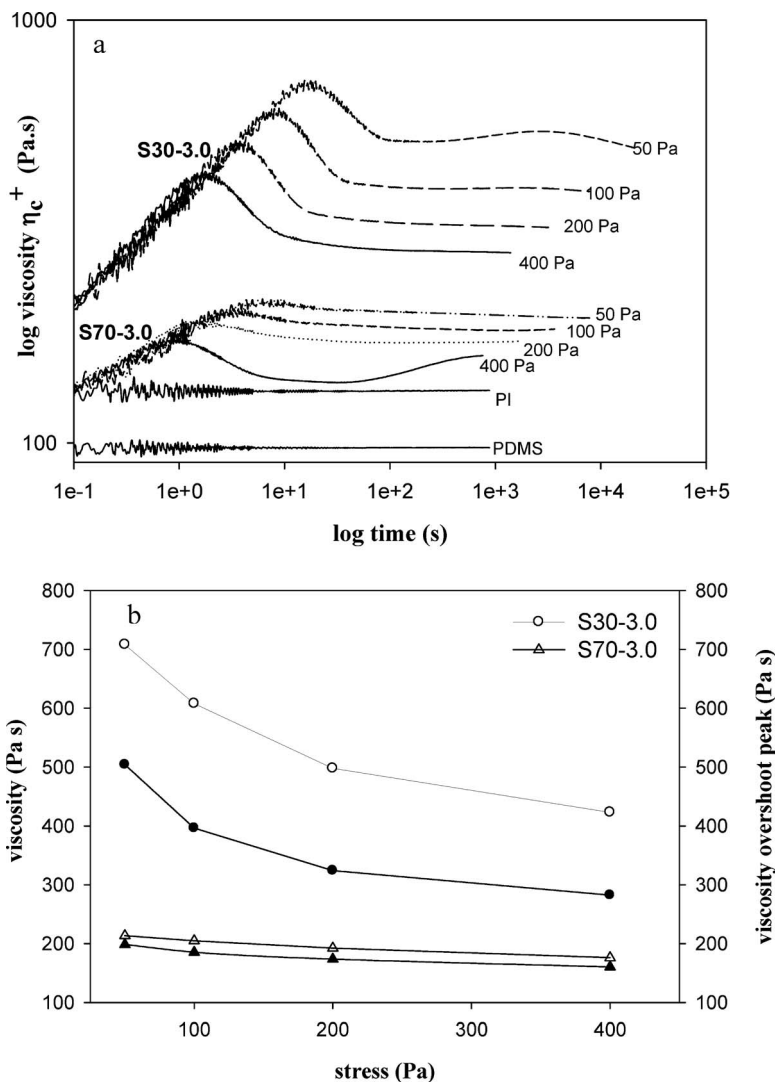


**FIG. 10.** (a) Shear viscosity after successive stepdowns in stress (400–50 Pa) of S30-3.0 and S70-3.0. Both blends show shear-thinning behavior and viscosity overshoots during the start-up of shearing. (b) Steady shear viscosity (closed symbols) and viscosity overshoot peak magnitude as functions of stress (open symbols) of S30-3.0 and S70-3.0.

Finally, we have also conducted limited experiments on S50-3.0 (data not shown) which has a far higher steady shear viscosity, as well as a far higher  $G'$  and  $|\eta^*|$  at low frequency. The morphology of S50-3.0 was not a simple droplet-matrix morphology and displayed very large droplet clusters. In summary, the compatibilizer effects on the rheological properties depend severely on the morphology: In blends with compositions closer to 50/50 and with extensive drop aggregation, processibility may be compromised.

#### IV. SUMMARY AND DISCUSSION

We first summarize the chief observations. Previously we had examined blends with a crosslinked reactive compatibilizer at a single compatibilizer loading (1.5%) and at a

single composition (30% PDMS in 70% PI). The focus of that article was comparing the crosslinked compatibilizer against a diblock. The chief focus of this paper on the other hand was to examine the effect of compatibilizer loading, in blends of two different compositions (30% PDMS in 70% PI and 30% PI in 70% PDMS).

The results of varying the compatibilizer loading are broadly as expected: At low compatibilizer loadings the behavior of the blend approaches that of the uncompatibilized blend. Even at the lowest compatibilizer loading, the linear viscoelastic properties showed a single interfacial relaxation (as compared to two relaxations for a diblock-containing blend). This indicates that the crosslinked compatibilizer, which forms a soft solidlike interface, cannot be described by a spreading pressure and does not possess dilational elasticity.

The results of varying the composition, however, were unexpected—at least three asymmetries were noted: (1) In S30 blends, the PDMS drops can stick to each other [Fig. 3(b)]. If such drops do coalesce [Fig. 3(a)], they can form nonspherical drops. In contrast, in S70 blends, the PI drops do not stick: They can coalesce, and the coalesced drops are spherical. (2) With regard to the dynamic oscillatory data, liquidlike behavior is observed in the S70 blends, while gel-like behavior, manifested by an increase in  $G'$  at low frequencies, was observed in the S30 blends. (3) The steady shear viscosity of the S70 blend, as well as the magnitude of the viscosity overshoots, was significantly lower than the S30 blend.

The rheological behavior appears to be entirely correlated with the sticking behavior: Most importantly the gel-like behavior and the viscosity overshoot of the S30 samples occur due to the large-scale aggregation of the PDMS drops in the S30 blends. Vice versa, the apparently normal behavior of the S70 blends is attributable to the fact that PI drops in PDMS do *not* stick to each other. Thus, the key issue is not the rheological asymmetry *per se*, but the underlying structural asymmetry, and we discuss it in greater detail.

What explains this structural asymmetry? On a macroscopic level, the viscosity mismatch between PI (130 Pa s) and PDMS (90 Pa s) creates some asymmetry, yet it appears to be too small to explain the above differences. On a molecular level, however, the architecture of the interfacially formed compatibilizer is not symmetric. The architecture of the compatibilizer is determined mainly by the structure of the reactive chains and by the mixing process. Table II lists some of the important molecular parameters on each side of the interface. Based on these numbers, and assuming that the reaction goes to completion (i.e., all the maleic anhydride reacts), we may schematically draw the structure of the interface illustrated in Fig. 11. The key features of this structure are:

- (1) the PI side of the interface is mostly loops and only a few tails (due to  $\sim 5$  reacted groups per chain), whereas the PDMS side has relatively few loops and mostly tails (due to the  $\sim 1$  reacted group per chain);
- (2) the PI side of the interface has much longer loops/tails than the PDMS side suggesting a thicker steric layer bound to the interface on the PI side; and
- (3) on the PI side, the homopolymer MW is about 7.5 times that of the loop molecular weight, whereas on the PDMS side the homopolymer MW is over 50 times that of the loop or tail MW. This situation when the homopolymer is much longer than the interfacially tethered polymer is called a dry brush (i.e., the homopolymer is excluded from the interfacially adsorbed brush). In that context, both sides are dry brushes, but the PDMS side is especially so [Fleer (1993); Lipatov and Nesterov (1997)].

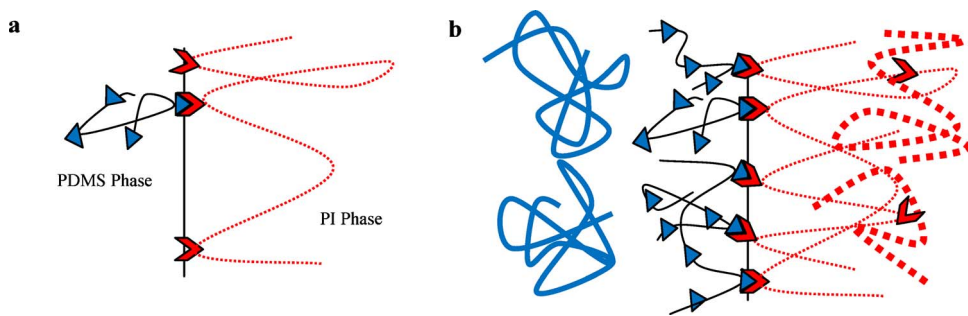


**FIG. 11.** Interfacially crosslinked compatibilizer showing (a) a single reacted chain of the reactive species on each side of the interface and (b) several reactive chains along with homopolymers chains. Thin chains represent interfacially reacted chains, whereas thick chains are the homopolymers. In (a), note the loops on the PI side of the interface and the tails on the PDMS side. In (b), note the complete exclusion of the PDMS homopolymer chains from the interfacially tethered PDMS chains (dry brush conditions). In contrast, the PI side of the interface may have some interpenetration.

Such asymmetry may be expected to affect coalescence behavior. Specifically, in cases when a block copolymer suppresses coalescence, the key mechanism is believed to be the steric hindrance of the block [Sundararaj *et al.* (1992); Macosko and Guegan (1996); Milner and Xi (1996)]. It has been observed that the effectiveness in suppressing coalescence increases with the length of the block, presumably because a longer and more swollen block can suppress coalescence more effectively [Lyu *et al.* (2002); Van Hemelrijck *et al.* (2005)]. The numbers in Table II suggest that coalescence should be suppressed more effectively in the S30 blends (PDMS drops in PI) than in S70 blends (PI drops in PDMS). This is indeed observed experimentally, i.e., the asymmetry in coalescence suppression may be explained based on the asymmetry in the loop length.

Explaining the asymmetry in sticking behavior is more challenging. At first glance, sticking appears to result from two phenomena: (1) Drops attract each other under quiescent conditions (due to van der Waals forces), but (2) cannot coalesce because they are covered with a crosslinked skin. Therefore, they stick to each other, similar to aggregation of solid particles dispersed in a polymer matrix. A significant difference is that because the drops can deform, they can stick more strongly than rigid particles, analogous to the strong adhesion between low-modulus solids as explained by the Johnson-Kendall-Roberts (JKR) theory [Packham (2005)]. This explanation can readily explain the sticking of PDMS drops in the S30-3.0 blend [Fig. 3(b)]. It can even explain the coalescence behavior of the S30-0.6 blend: In that case we speculate that the crosslinked skin is not sufficiently robust and it ruptures, thus permitting coalescence. However, since a crosslinked compatibilizer cannot desorb from the interface, the resulting drops do not recover spherical shape [Fig. 3(a)]. Nonetheless, this explanation cannot explain the apparently normal behavior of the reactively compatibilized S70 blends. In particular, it cannot explain why—even though PI drops in PDMS are covered with a crosslinked skin—they do not stick, do coalesce, and do remain spherical shapes under all quiescent conditions studied. It appears that the crosslinked skin in the S70 blends ruptures readily and, furthermore, is much more fluidlike than in the S30 blends. The reasons for this are not clear, specifically, why the crosslinked skin behaves like a soft solid when PI is the continuous phase, but not when PDMS is a continuous phase remains unknown.

## V. SUMMARY AND CONCLUSIONS

We have examined the effects of reactive compatibilizer concentration and homopolymer concentration in model blends of PI and PDMS using two multifunctional reactive species which create a crosslinked interface. Increasing reactive compatibilizer loading in PI-continuous (S30) blends was found to increase the formation of drop clusters and increase the “gel-like” behavior and viscosity of the blends. Contrarily, blends of PI dispersed in PDMS (S70) showed no droplet clusters or gel-like oscillatory behavior. Flow-induced coalescence was suppressed at compatibilizer loadings greater than 0.4% of the total weight in S30 blends. In S70 blends, coalescence occurred at all compatibilizer levels, although it slowed down with increasing compatibilizer loading.

We speculate that the differences in rheological behavior of the S30 vs S70 blends are entirely related to whether the drops stick and form clusters. The presence of clusters in the S30 blends is responsible for the gel-like oscillatory behavior, high steady shear viscosity, and the large viscosity overshoots in S30 blends. In contrast, the apparently normal behavior of the S70 blends seems to arise from the lack of clustering in these blends.

While the architecture of the crosslinked block copolymer is asymmetric on the two sides of the interface, it is not entirely clear why these asymmetries allow the PDMS drops in PI stick to each other but not the PI drops in PDMS. The mechanical properties of the interface appear to depend on which phase is continuous, and the reasons for this remain unknown.

## ACKNOWLEDGMENTS

We are grateful to the Laboratory of Applied Rheology at the Katholieke Universiteit Leuven for making the PI-PMDS diblock copolymer available for this research. We thank Rhodia Silicones and Kuraray Co. for providing the PDMS and PI homopolymers, respectively. We would also like to thank the Center for Biological Imaging at the University of Pittsburgh for the use of their microscopy facilities and Dr. Toby Chapman, University of Pittsburgh, for his advice regarding fluorescent labeling. This research was supported by IGERT Grant No. DGE-0504345 and CAREER Grant No. CBET-0448845 from the National Science Foundation.

## References

- Baker, W. E., C. E. Scott, and G. H. Hu, *Reactive Polymer Blending* (Hanser Gardner, Cincinnati, 2001).
- Beck Tan, N. C., S. K. Tai, and R. M. Briber, “Morphology control and interfacial reinforcement in reactive polystyrene/amorphous polyamide blends,” *Polymer* **37**(16), 3509–3519 (1996).
- Datta, S., and D. Lohse, *Polymeric Compatibilizers: Uses and Benefits in Polymer Blend* (Hanser, Vienna, 1996).
- DeLeo, C., and S. Velankar, “Morphology and rheology of compatibilized polymer blends: Diblock compatibilizers versus crosslinked reactive compatibilizers,” *J. Rheol.* **52**(6), 1385–1404 (2008).
- Doublier, J. L., and P. J. Wood, “Rheological properties of aqueous solutions of (1-3)(1-4)-beta-d-glucan from oats (*Avena-Sativa* L),” *Cereal Chem.* **72**(4), 335–340 (1995).
- Fager, R. S., C. B. Kutina, and E. W. Abrahamson, “The use of NBD chloride (7 chloro-4-nitrobenzo-2-oxa-1,3-diazole) in detecting amino acids and as an N-terminal reagent,” *Anal. Biochem.* **53**(1), 290–294 (1973).
- Fleer, G. J., *Polymers at Interfaces* (Chapman and Hall, London, 1993).
- Friedrich, C., and Y. Y. Antonov, “Interfacial relaxation in polymer blends and Gibbs elasticity,” *Macromol-*

- ecules **40**(4), 1283–1289 (2007).
- Gramespacher, H., and J. Meissner, “Interfacial tension between polymer melts measured by shear oscillations of their blends,” *J. Rheol.* **36**(6), 1127–1141 (1992).
- Hu, Y. T., D. J. Pine, and G. L. Leal, “Drop deformation, breakup, and coalescence with compatibilizer,” *Phys. Fluids* **12**(3), 484–489 (2000).
- Jacobs, U., M. Fahrlander, J. Winterhalter, and C. Friedrich, “Analysis of Palierne’s emulsion model in the case of viscoelastic interfacial properties,” *J. Rheol.* **43**(6), 1495–1509 (1999).
- Koning, C., M. Van Duin, C. Pagnoulle, and R. Jerome, “Strategies for compatibilization of polymer blends,” *Prog. Polym. Sci.* **23**, 707–757 (1998).
- Lin, Y., A. Boker, J. He, K. Sill, H. Xiang, C. Abetz, X. Li, J. Wang, T. Emrick, S. Long, Q. Wang, A. Balazs, and T. P. Russell, “Self-directed self-assembly of nanoparticle/copolymer mixtures,” *Nature (London)* **434**(7029), 55–59 (2005).
- Lipatov, Y. S., and A. E. Nesterov, *Interface in Demixing Solutions and Polymer Mixtures. Thermodynamics of Polymer Blends* (Technomic, Lancaster, PA, 1997).
- Lyu, S., T. D. Jones, F. S. Bates, and C. W. Macosko, “Role of block copolymers on suppression of droplet coalescence,” *Macromolecules* **35**, 7845–7855 (2002).
- Macosko, C. W., and P. Guegan, “Compatibilizers for melt blending: Premade block copolymers,” *Macromolecules* **29**(17), 5590–5598 (1996).
- Martin, J., and S. Velankar, “Effects of compatibilizer on immiscible polymer blends near phase inversion,” *J. Rheol.* **51**(4), 669–692 (2007).
- Milner, S. T., and H. Xi, “How copolymers promote mixing of immiscible homopolymers,” *J. Rheol.* **40**(4), 663–687 (1996).
- Mohanty, A. K., M. Misra, and L. T. Drzal, “Sustainable bio-composites from renewable resources: Opportunities and challenges in the green materials world,” *J. Polym. Environ.* **10**(1–2), 19–26 (2002).
- Oldroyd, J., “The elastic and viscous properties of emulsions and suspensions,” *Proc. R. Soc. London, Ser. A* **218**(1132), 122–132 (1953).
- Oshinski, A. J., H. Keskkula, and D. R. Paul, “Rubber toughening of polyamides with functionalized block copolymers: 2. Nylon-6,6,” *Polymer* **33**(2), 284–293 (1992).
- Oshinski, A. J., H. Keskkula, and D. R. Paul, “The effect of polyamide end-group configuration on morphology and toughness of blends with maleated elastomers,” *J. Appl. Polym. Sci.* **61**(4), 623–640 (1996).
- Packham, D. E., *Handbook of Adhesion* (Wiley, West Sussex, 2005).
- Palierne, J. F., “Linear rheology of viscoelastic emulsions with interfacial tension,” *Rheol. Acta* **29**, 204–214 (1990).
- Pozo, O., D. Collin, H. Finkelmann, D. Rogez, and P. Martinoty, “Gel-like elasticity in glass-forming side-chain liquid-crystal polymers,” *Phys. Rev. E* **80**(3), 031801 (2009).
- Riemann, R. E., H. J. Cantow, and C. Friedrich, “Interpretation of a new interface-governed relaxation process in compatibilized polymer blends,” *Macromolecules* **30**(18), 5476–5484 (1997).
- Ross-Murphy, S. B., “Structure-property relationships in food biopolymer gels and solutions,” *J. Rheol.* **39**(6), 1451–1463 (1995).
- Sun, Y.-J., R. J. G. Willemsse, T. M. Liu, and W. E. Baker, “*In situ* compatibilization of polyolefin and polystyrene using Friedel–Crafts alkylation through reactive extrusion,” *Polymer* **39**(11), 2201–2208 (1998).
- Sundararaj, U., C. W. Macosko, R. J. Rolando, and H. T. Chan, “Morphology development in polymer blends,” *Polym. Eng. Sci.* **32**(24), 1814–1823 (1992).
- Thareja, P., and S. S. Velankar, “Particle-induced bridging in immiscible polymer blends,” *Rheol. Acta* **46**(3), 405–412 (2007).
- Tselios, C., D. Bikiaris, V. Maslis, and C. Panayiotou, “*In situ* compatibilization of polypropylene-polyethylene blends: A thermomechanical and spectroscopic study,” *Polymer* **39**(26), 6807–6817 (1998).
- Van Hemelrijck, E., P. Van Puyvelde, C. W. Macosko, and P. Moldenaers, “The effect of block copolymer architecture on the coalescence and interfacial elasticity in compatibilized polymer blends,” *J. Rheol.* **49**(3), 783–798 (2005).
- Van Hemelrijck, E., P. Van Puyvelde, and P. Moldenaers, “Rheology and morphology of highly compatibilized

- polymer blends," *Macromol. Symp.* **233**, 51–58 (2006).
- Van Hemelrijck, E., P. Van Puyvelde, S. Velankar, C. W. Macosko, and P. Moldenaers, "Interfacial elasticity and coalescence suppression in compatibilized polymer blends," *J. Rheol.* **48**(1), 143–158 (2004).
- Van Puyvelde, P., S. Velankar, and P. Moldenaers, "Rheology and morphology of compatibilized polymer blends," *Curr. Opin. Colloid Interface Sci.* **6**, 457–463 (2001).
- Velankar, S., P. Van Puyvelde, J. Mewis, and P. Moldenaers, "Steady-shear rheological properties of model compatibilized blends," *J. Rheol.* **48**(4), 725–744 (2004).
- Vinckier, I., P. Moldenaers, and J. Mewis, "Relationship between rheology and morphology of model blends in steady shear flow," *J. Rheol.* **40**(4), 613–631 (1996).
- R. A. Weiss, C. Beretta, S. Sasongko, and A. Garton, "Miscibility enhancement of polystyrene and poly(alkylene oxide) blends using specific intermolecular interactions," *J. Appl. Polym. Sci.* **41**, 91–103 (1989).
- Winter, H. H., and F. Chambon, "Analysis of linear viscoelasticity of a cross-linking polymer at the gel point," *J. Rheol.* **30**(2), 367–382 (1986).